Supporting Information:

Near-Field Manipulation in a Scanning Tunneling Microscope Junction with Plasmonic Fabry-Pérot Tips

Hannes Böckmann[1†], Shuyi Liu[1†], Melanie Müller[1], Adnan Hammud[2], Martin Wolf[1], Takashi Kumagai[1,3]*

[1]*Department of Physical Chemistry, Fritz-Haber Institute of the Max-Planck Society, Faradayweg 4-6, 14195 Berlin, Germany.*

[2]*Department of Inorganic Chemistry, Fritz-Haber Institute of the Max-Planck Society, Faradayweg 4-6, 14195 Berlin, Germany.*

[3]*JST-PRESTO, 4-1-8 Honcho, Kawaguchi, Saitama 332-0012, Japan.*

*Corresponding author: kuma@fhi-berlin.mpg.de

[†]These authors equally contributed.

1. FIB fabrication of the Au tips

The FIB fabrication of electrochemically-etched Au tips was performed an FEI Helios NanoLab G3 FIB-SEM DualBeam system and Ga ions were used. It provides Gallium ions with an acceleration voltage up to 30 kV and enables milling and deposition of structures with critical dimensions of less than 10 nm. The tips were mounted on a pre-tilted specimen holder and oriented towards the ion beam such that the axis of the tip is collinear with the ion beam. We performed a multiple-step annular milling process with different parameters and a varying order, depending on the initial tip profile and the required sharpened length. Taking into account the re-deposition dynamics during ion milling and the fact, that the main re-deposition of removed material occurs underneath the ion beam incidence point at highly steep surfaces, we preferred an inner-to-outer-radius scan direction, *i.e.*, from the apex downwards, in order to simultaneously remove re-deposited material.

Several tip fabrication procedures using FIB milling were already suggested before.[1, 2] Here we introduce a similar procedure with a reverse milling sequence and different parameters. We first start the tip fabrication with a low ion energy step at 5 kV in order to shape and smoothen the apex. Subsequently, we increase the inner and outer radii as well as the ion energy and beam current to obtain higher milling rates to only sharpen the shaft to the required length. This step order aims to minimize damage and Gallium implantation into the apex and in close vicinity to it. Finally, we apply a low energy polishing step at 5 kV to the sharpened length of the shaft to reduce damage layer caused by 30 kV ions.

A key parameter in ion milling processes is the volume per dose value ΔV, i.e. the removed material volume per primary ion. It is material-specific and determines, at a certain ion energy, the milling time t for a required depth Z and a given beam current I:

$$\Delta V = \frac{\text{Volume}}{\text{Charge}} = \frac{X \times Y \times Z}{I \times t}$$

For the groove fabrication and in order to precisely control the groove depth Z and the milling time t, we set this value to 1.5 µm³/ nC and 0.42 µm³/ nC for Au and Ag, respectively, [3] and used, at 30 kV ion energy, the lowest ion beam current of ca. 7 pA to avoid excessive milling and thus damaging the apex.

2. Peak position analysis in the bias voltage-dependent STML spectra

Figure S1 shows Multi-peak fitting analysis of the bias voltage-dependent STML spectra in **Fig. 2c**. It appears that a slight blue-shift is observed at long wavelengths (peak number 4 and 5). As shown below (**Fig. S2**), the peak positions remain almost identical in the current-dependent STML spectra where the tip–surface distance is also changed. Therefore, the blue-shift in the voltage-dependent STML spectra may not be related to the gap distance. As seen in **Fig. 1** (the voltage-dependent STML spectra for a non-groove tip), the applied voltage determines the quantum cutoff of the LSPR excitation and affects the overall spectral response. The different spectral feature of the LSP may lead to different coupling to the propagating SPP modes.

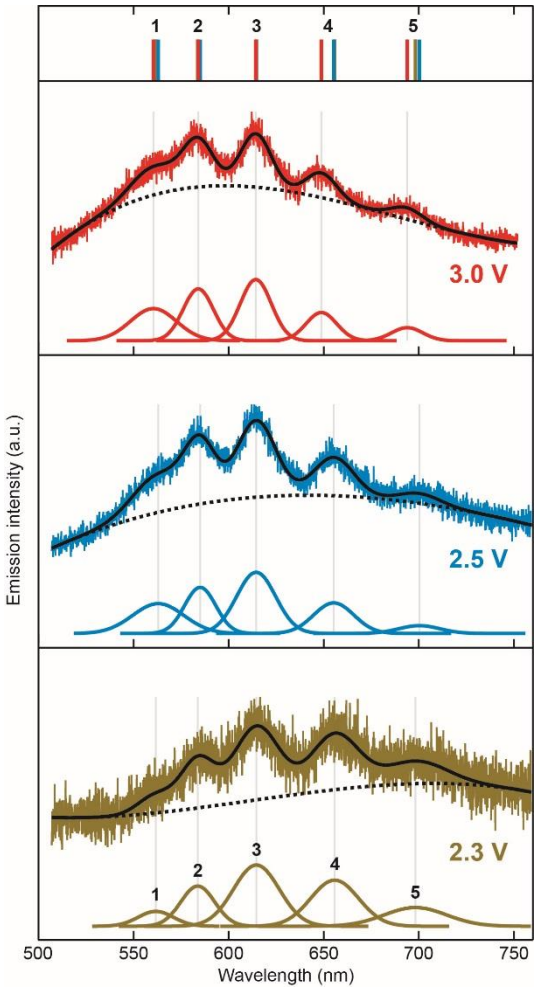

Figure S1. Multi-peak fitting analysis of the bias voltage-dependent STML spectra in **Fig. 2C**. The data are fitted using Gaussian functions (solid lines) with a cubic background (dashed lines). The top panel shows the peak positions.

3. Current dependence of the STML intensity for the grooved tip

The luminescence intensity at 615 nm for the 3-μm grooved tip (**Fig. 2d**) is plotted as a function of the tunneling current, indicating a linear dependence.

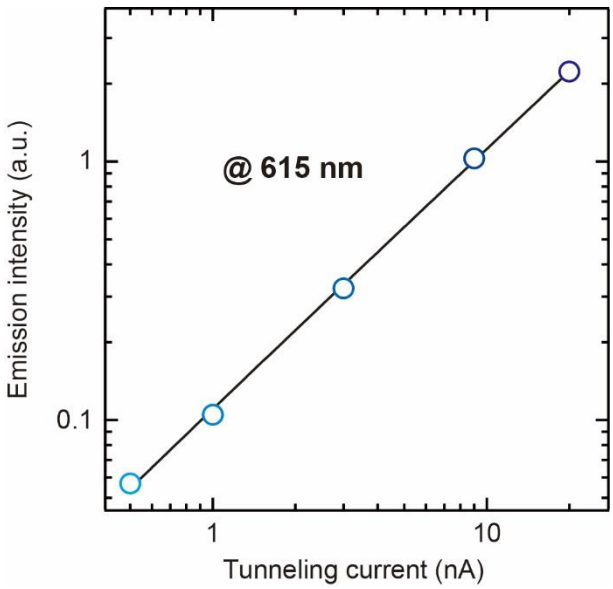

Figure S2. Peak intensity at 614 nm of the STML spectra in **Fig. 2d** is plotted as a function of the tunneling current. The black line indicates the linear fitting result.

4. Numerical simulation of electromagnetic field distributions

Numerical simulations were performed to calculate the plasmonic response of the nanotip and STM-junction by solving the time-harmonic wave equation for the electric field within the RF-Module of COMSOL Multiphysics 5.3a. Simulations are performed in 3D for a groove distance of L = 3 µm (although the problem is fully radially symmetric, simulations needed to be performed in 3D as the point dipole excitation feature is not available in 2D radially symmetric models in COMSOL 5.3a). The structural parameters of the tip were taken from the SEM micrograph (**Fig. 2b**). The width of the simulation volume is 1.3 µm and the tip is truncated above the groove at 4 µm distance from the apex. Except for the 100 nm thick sample, which is chosen thick enough to not transmit any fields, the simulation volume is surrounded by perfectly matched layers to absorb all outgoing waves.

For a given excitation frequency and dipole current amplitude, COMSOL then solves for the full time-harmonic electromagnetic field distribution. Simulations are performed for excitation wavelength between 500–750 nm in 5 nm steps. The materials properties are set by the complex dielectric functions of gold and silver, with the values taken from the Lorentz-Drude model. Specifically, the Drude-Lorenz parameters used are taken from Ref. 4. Without a groove, a smooth distribution of the electric field amplitude is observed at the tip shaft without a standing wave pattern. Introducing the groove structure causes reflection of propagating surface plasmon polaritons and a modulation of the electric field amplitude due to the resulting SPP standing wave, as depicted in **Fig. 2e**.

References

[1]Vasile, M. J.; Grigg, D.; Griffith, J. E.; Fitzgerald, E.; Russell, P. E. Scanning probe tip geometry optimized for metrology by focused ion beam ion milling, Microelectronics and Nanometer Structures Processing, Measurement, and Phenomena. *J. Vac. Sci. Technol.* B **1991** *9*, 3569.

[2] Wang, Z. M. FIB Nanostructures, Lecture Notes in Nanoscale 1, Science and Technology 20, Springer International Publishing Switzerland 2013; DOI 10.1007/978-3-319-02874-3

[3] Orloff, J; Swanson, L. W.; Utlaut, M. High Resolution Focused Ion Beams: FIB and its Applications, Springer Science + Business Media New York 2003; DOI 10.1007/978-1-4615-0765-9

[4] Rakić, A. D.; Djurišić, A. B.; Elazar, J. M.; Majewski, M. L. Optical properties of metallic films for vertical-cavity optoelectronic devices. *Appl. Opt.* **1998**, *37*, 5271–5283.